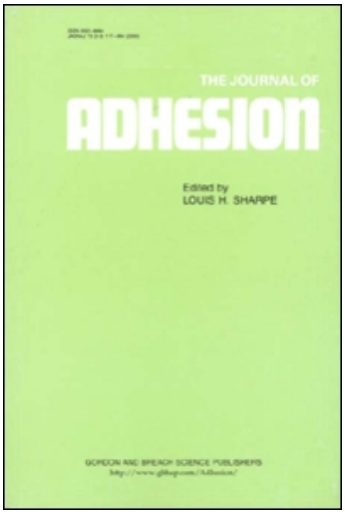

The Journal of Adhesion
Publication details, including instructions for authors and subscription information:
http://www.informaworld.com/smpp/title~content=t713453635

Measuring Hydro-Static Dependent Constitutive Behaviour of Adhesives Using a Bend Specimen

A. D. Crocombe[a]; G. Richardson[a]; P. A. Smith[b]
[a] Dept of Mechanical Engineering, University of Surrey, Guildford, Surrey, UK [b] Dept Materials Science and Engineering, University of Surrey, Guildford, Surrey, UK

To cite this Article Crocombe, A. D. , Richardson, G. and Smith, P. A.(1993) 'Measuring Hydro-Static Dependent Constitutive Behaviour of Adhesives Using a Bend Specimen', The Journal of Adhesion, 42: 3, 209 — 223
To link to this Article: DOI: 10.1080/00218469308044648
URL: http://dx.doi.org/10.1080/00218469308044648

J. Adhesion, 1993, Vol. 42, pp. 209–223
Reprints available directly from the publisher
Photocopying permitted by license only

Printed in the United States of America.

Measuring Hydro-Static Dependent Constitutive Behaviour of Adhesives Using a Bend Specimen*

A. D. CROCOMBE and G. RICHARDSON

Dept of Mechanical Engineering, University of Surrey, Guildford, Surrey, GU2 5XH, UK

P. A. SMITH

Dept Materials Science and Engineering, University of Surrey, Guildford, Surrey, GU2 5XH, UK

(Received July 27, 1992; in final form February 11, 1993)

A simple bend test and associated equations that determine, simultaneously, both the tensile and compressive uniaxial stress-strain behaviour of a bulk adhesive are presented. From this, the ratio of the flow stress in compression to tension (S) can be found. Such data are required if a meaningful elasto-plastic stress analysis of an adhesive joint is to be carried out. Experimental results for both the tensile and compressive stress-strain data are obtained for an epoxy specimen using this technique. The tensile data are compared with the results from uniaxial tensile tests on flat dumbell specimens of the same material and the good correlation that is found indicates that this is a reliable technique. Values of the ratio (S) for this adhesive are calculated as a function of both strain hardening and work hardening parameters. These results indicate that this technique complements standard test techniques and provides an elegant method not only of obtaining the ratio (S) but also of deriving uniaxial stress-strain curves.

KEY WORDS adhesive properties; flexural test; tensile tests; hydrostatic stress sensitive yield criteria; rate dependency; reconstitution of data.

NOTATION

Symbols:

δ —mid-span deflection
D —distance between the anvils
Δ —vertical displacement of the anvils
E —tensile modulus
ϵ —uniaxial strain
J —stress invariant
κ —hardening parameter
L —span between outer anvils
M—bending moment/unit width
R —radius of the anvil
S —ratio of compressive to tensile flow stress
σ —uniaxial stress

Subscripts:

1 —first stress invariant
2 —second stress invariant
c —compressive
d —of defined material behaviour
e —effective
ϵ —strain hardening
i, i − 1—the current and previous loading increment
max —maximum value
p —plastic
t —tensile
u —of undefined material behaviour
w —work hardening

*Presented at The Plastics and Rubber Institute Conference, "Structural Adhesives in Engineering III," at Bristol University, Bristol, England, 30 June–2 July, 1992.

NOTATION

Symbols:

T —tensile force/unit width
t —section thickness
W—specimen width
ω —thickness carrying stresses in excess of known values
y —distance from the neutral axis

INTRODUCTION

A necessary step in a successful stress analysis of an adhesive joint is the evaluation of the constitutive properties of the adhesive concerned. Where failure in the joint is interfacial then it is also necessary to have data characterising the interface. However, the present work is concerned only with evaluating the adhesive constitutive properties. The amount of data that is required depends on the complexity of the stress analysis being undertaken. It is generally recognised[1] that to carry out a meaningful analysis, particularly with a tough or ductile adhesive, elasto-plastic behaviour should be included. When such an analysis is being carried out, in addition to the basic linear-elastic properties of the adhesive such as the tensile modulus and Poisson's ratio it is also necessary to have data defining the onset and subsequent growth of yielded material. These are usually provided in the form of a non-linear stress strain curve that contains a yield point (onset of permanent deformation) and post-yield behaviour. This is illustrated schematically in Figure 1. For adhesives, such a curve is usually found from a simple test such as a tensile test of the adhesive[2] or a thick lap shear test[3] on a joint. In an analysis of an adhesive joint, the adhesive generally experiences a combined state of stress and this can be related to an appropriate point on the stress strain curve by evaluating an "effective" uniaxial tensile stress that is equivalent to the combined stress state. For metals this effective stress is a function only of the deviatoric stress or the second stress invariant (J_{2d}) (this causes a change of shape only) and a common expression for the effective stress (σ_e) is

$$\sigma_e = (3J_{2d})^{1/2} \tag{1}$$

However, for adhesives (as for other polymers) it has been found that the effective stress is a function not only of the deviatoric stress but also of the hydrostatic stress or the first stress invariant (J_1) (this causes a change in volume). Various formulae have been derived for the effective stress as a function of the first and second stress invariants, two of which are shown below. The first was adapted from Raghava and Cadell[4] by Peppiat[5] and the second is presented in work by Gali *et al.*[6]

$$\sigma_e = [J_1(S-1) + (J_1^2(S-1)^2 + 12J_{2d}S)^{1/2}]/2S \tag{2}$$

or

$$\sigma_e = [J_1(S-1) + (S+1)\,(3J_{2d})^{1/2}]/2S \tag{3}$$

Although the forms of these equations are slightly different it can be seen that they both include a parameter S. This is defined as the ratio of yield stress and subsequent flow stress obtained from uniaxial compression and tension tests, respectively. Thus,

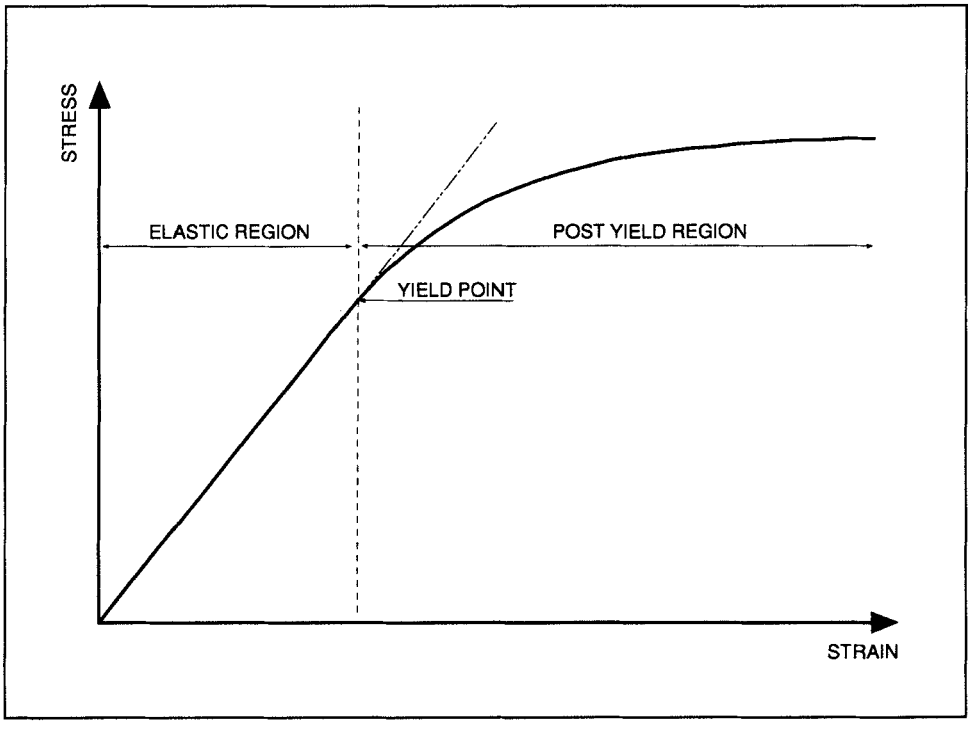

FIGURE 1 Schematic representation of the stress-strain curve.

an additional material parameter has been introduced and needs to be evaluated for each adhesive, as well as the complete uniaxial tensile stress curve. In the past it has been necessary to carry out tensile tests on carefully manufactured and instrumented specimens of adhesive and also supplementary compressive tests to determine these data.

This paper presents a single test that not only provides the required material information but also is considerably simpler to carry out than the tensile test. It also achieves higher strains to failure than the tensile test (although these strains are still lower than the strains in some adhesive joints). The technique is based on the four-point bend specimen. Four-point bend tests have been used in the past[7] to evaluate material properties such as the tensile modulus and yield point of a material. However, to the authors knowledge, it has not been used to reconstitute the complete non-linear uniaxial stress-strain curve and has certainly not been used for this purpose when the tensile and compressive stress-strain curves are different, as is the case for polymers where the yielding is affected by the hydrostatic stress. Both tensile and compressive strain data are measured within the gauge length at increasing values of applied moments. By assuming that the strain distribution remains linear across the section, equations can be developed that can be used in an incremental manner to convert the moment-strain data into both tensile and compressive stress-strain curves. Although the resulting curves are not as accurate as the pure uniaxial data it will be shown that reasonable correlation exists.

The next section presents the derivation of the equations that are needed to reconstitute the tensile and compressive stress-strain curves from the recorded surface strains and the associated moment. This is followed by a description of the experimental procedure. Results are then processed and presented for an epoxy adhesive. These are compared with data from independent tensile tests and the paper concludes with a discussion of the technique and an assessment of the errors involved.

THEORY

In this section mathematical relationships are developed which enable tensile and compressive material behaviour to be obtained from the results of a four-point bend test carried out on a strip of cured adhesive that has a rectangular cross section. The equations are developed for a rate-insensitive material in which plastic flow occurs at a constant volume. At the end of the paper the implications of applying this technique to typical rate-dependent materials are considered.

The bending moment (M) and tension (T) at any section can be defined in terms of the stress (σ), strain (ϵ) and distance (y) from the section's neutral axis as

$$M = \int_t y\sigma(\epsilon)\, dy \tag{4}$$

$$T = \int_t \sigma(\epsilon)\, dy \tag{5}$$

It should be noted that the tensile load (T) is normally zero and that, in general, the tensile and compressive stress-strain curves will not be the same. Thus, by considering the tensile and compressive stress-strain behaviour separately, equations 4 and 5 can be rewritten in terms of integrals over the portions of the thickness that are subject to tensile (t_t) and compressive (t_c) stresses respectively.

$$M = \int_{t_t} y\sigma_t(\epsilon)\, dy + \int_{t_c} y\sigma_c(\epsilon)\, dy \tag{6}$$

$$T = \int_{t_t} \sigma_t(\epsilon)\, dy + \int_{t_c} \sigma_c(\epsilon)\, dy \tag{7}$$

Since the specimen is in bending, the strain (ϵ) at any point across the section can be assumed to vary linearly and can be written in terms of the surface strains ϵ_t and ϵ_c.

$$\epsilon = \frac{\epsilon_t - \epsilon_c}{t} y \tag{8}$$

Experimentally, ϵ_t and ϵ_c can be obtained as a function of applied moment. To obtain $\sigma_t(\epsilon)$ and $\sigma_c(\epsilon)$ (and thus the tensile and compressive constitutive relations) from these data an incremental procedure is used. The rearrangement of equations

6, 7 and 8 into incremental form is outlined in the Appendix and leads to equations 9 and 10 below. These express the tensile and compressive stresses corresponding to the ith moment increment in terms of moments at this and the previous increment, the stresses at the previous increment and the thicknesses of the section (ω_{ti} and ω_{ci}) that are subject to stresses (tensile and compressive, respectively) that are greater than those measured in the previous increment

$$\sigma_{t(i)} = \frac{M_i - M_{i-1}\left[1 - \frac{\omega_{t(i)} + \omega_{c(i)}}{t}\right]^2 + \sigma_{t(i-1)}\omega_{t(i)}\left[\frac{t}{2} - \frac{\omega_{t(i)}}{3} - \frac{\omega_{c(i)}}{6}\right] - \sigma_{c(i-1)}\frac{\omega_{c(i)}^2}{6}}{\frac{\omega_{t(i)}}{2}\left[t - \frac{\omega_{t(i)} + \omega_{c(i)}}{3}\right]} \tag{9}$$

$$\sigma_{c(i)} = \frac{-1}{\omega_{c(i)}}\left[\sigma_{t(i-1)}\omega_{t(i)} + \sigma_{c(i-1)}\omega_{c(i)} + \sigma_{t(i)}\omega_{t(i)}\right]. \tag{10}$$

The values of ω_{ti} and ω_{ci} can be found from the known linear strain distribution as

$$\omega_{t(i)} = \frac{t}{(\epsilon_{t(i)} - \epsilon_{c(i)})} \cdot |\epsilon_{t(i)} - \epsilon_{t(i-1)}| \tag{11}$$

$$\omega_{c(i)} = \frac{t}{(\epsilon_{t(i)} - \epsilon_{c(i)})} \cdot |\epsilon_{c(i)} - \epsilon_{c(i-1)}| \tag{12}$$

The values of the surface tensile and compressive stresses that correspond to the surface strains measured during a given load increment are determined by using equations 9 to 12 above. This process can be repeated for all the increments of loading, yielding full tensile and compressive stress-strain data. Using these two curves, S can be determined as a function of a hardening parameter κ. Two different definitions for hardening are assumed, strain and work hardening and the value of S corresponding to both can be found.

For plastic flow governed by strain hardening the hardening parameter can be defined in terms of the stresses and elastic tensile modulus (E) as

$$\kappa_\epsilon = \epsilon_p = \epsilon - \sigma/E \tag{13}$$

For work hardening the parameter can be defined as

$$\kappa_\omega = \int \sigma \, d\epsilon_p \tag{14}$$

this can be written in incremental form as

$$\kappa_i = \kappa_{i-1} + \frac{\sigma_i + \sigma_{i-1}}{2}(\epsilon_{pi} - \epsilon_{pi-1}) \tag{15}$$

By determining κ at each ϵ point the stress-strain curves can be converted into stress-hardening parameter curves. These curves can be used to find the compressive and tensile stresses at a given value of the hardening parameter. Dividing the compressive stress by the tensile stress gives the ratio S for that value of κ *i.e.*

$$S(\kappa) = \frac{\sigma_c(\kappa)}{\sigma_t(\kappa)} \tag{16}$$

TEST DESCRIPTION

This section presents the basic test geometry used to implement the incremental analysis derived in the last section and describes also how the tests were carried out. Figure 2 shows the dimensions of the adhesive specimen and details of the points of application of the load. Note that a relatively thick specimen was used. This thickness is something of a compromise; if it is too small, then the deflection of the specimen becomes excessive and slipping occurs on the anvils while, if it is too large, then the applied loads can cause local deformation and produce an unacceptable variation of surface stress (which is normally assumed to be constant) over the centre section. In this work the ratio of the maximum mid-span displacement to span length (δ_{max}/L) was less than 0.1 and this did not pose any undue problems with regard to slipping round the anvils and corrections for rotation. It is difficult to calculate the required thickness to give such a ratio as the maximum surface strains (ϵ_{max}) are generally not known. Thus a method of trial and error is probably more appropriate. However, by making a number of elementary assumptions about the geometry of

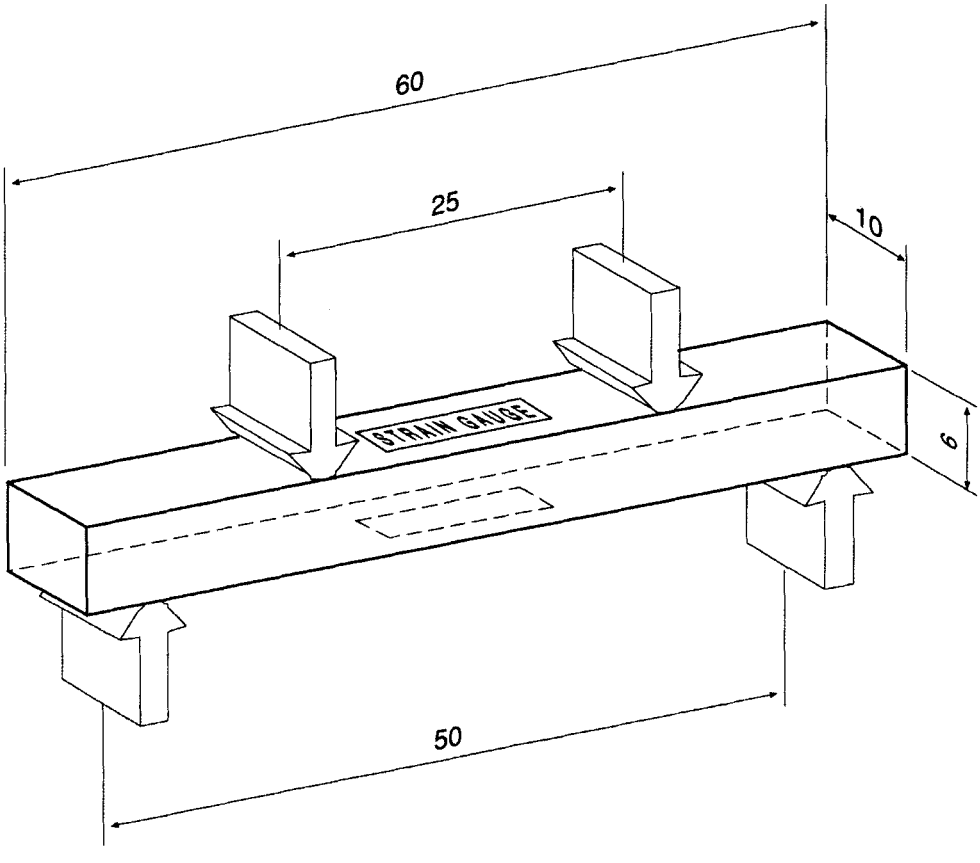

FIGURE 2 Geometry of the four-point bend test sample.

the deformed beam an approximate value for the thickness (t) is

$$t = \frac{11}{48} L \epsilon_{max} \frac{L}{\delta_{max}} \tag{17}$$

From this equation it can be seen that the required thickness increases with the maximum surface strain. In practice the thickness can only be increased to a certain level as edge effects will affect the stress distribution between the inner anvils. Linear finite element analysis has shown that when the thickness is 25% of the total span there is about a 3% variation in stress over the centre half of the inner span. It is suggested that this thickness-to-span ratio should be taken as an upper limit. A value of 25% of the inner span has been cited as a reasonable value elsewhere.[7] For thicker specimens, however, the value of the applied load will increase and may cause permanent damage of the surface. Thus, the recommendation is to use the smallest thickness that will give a reasonable value of the deflection/span ratio. No permanent deformation under the anvils was noted in the specimens used in this work.

A schematic representation of the test set-up is shown in Figure 3. The specimen is supported initially on outer anvils that are fixed to the moving crosshead on an Instron 6025, a servo electro-mechanical universal testing machine. The load is applied to the specimen by driving the crosshead upwards at a given speed, thus bringing the specimen into contact with the fixed inner anvils. These are located directly on the load cell which outputs an instantaneous value of the load. From this load the moment applied over the inner section of the strip can be found. For this experimental work the crosshead speed was held constant at 0.1 mm/min. This produced

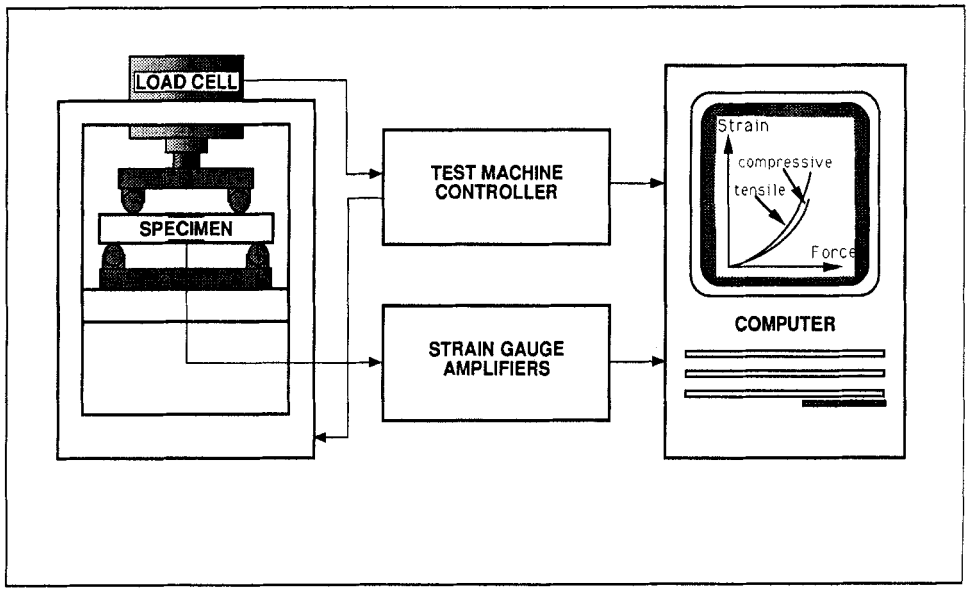

FIGURE 3 Schematic diagram of the experimental apparatus.

a strain rate on the surface of the adhesive that varied between 0.1 and 0.25 %/min. The surface strains that are required to implement the incremental analysis derived in the last section are measured using strain gauges bonded to the upper and lower surfaces of the inner span of the strip. Clearly, to carry out the analysis it is necessary to know the surface strains at given levels of applied load. To obtain smooth moment and strain curves a reasonable number of data points are required and, thus, a decision was made to automate the strain and load measuring procedure. This is illustrated schematically in Figure 3 where it can be seen that a voltage output from the load cell and from the strain gauge processing instrumentation are fed into a Macintosh computer that is running a software programme that was specifically written to aid data capture and display. The data captured using this package can be displayed on the screen in graphical format or read into a spreadsheet package where the incremental analysis was carried out. The spreadsheet was developed to implement the incremental analysis and produce tensile and compressive stress-strain curves. It should be emphasised that the analysis could be carried out using any programming language and the spreadsheet was only used for convenience.

The specimens themselves were manufactured in bulk form through the use of a mould which consisted of a top and bottom plate separated by spacers of the appropriate thickness and sealed around the perimeter using a flexible tape. Prior to assembling the mould the spacing pieces were coated with mould release spray and Melinex (polyester) sheets were attached to the top and bottom plates with a very thin layer of silicone adhesive. The Melinex gave a smooth surface finish to the adhesive strips. The particular adhesive used for the experimental work was a two-part cold cure adhesive supplied by Permabond. It was unfilled and was relatively inviscid which meant that, after careful mixing and degassing, it could be dispensed into the mould using a syringe and wide-bored needle. The filled mould was left at 30°C for 24 hours and then dissembled and the adhesive specimen removed and stored in a dessicator until testing, except while bonding the strain gauges.

Strain gauging was carried out using TML standard single gauges from Techni Measure, UK, bonded with a cyanoacrylate adhesive. They had a 6 mm grid size, 120 ohm resistance and pre-soldered lead wires. Although there was a potential problem with local heating it was found that the strain recorded (using a quarter bridge) on an unloaded specimen did not vary with time and this implies that there is no significant heating effect (which would affect the resistance of the gauge). A terminal tag was bonded onto the specimen, adjacent to the strain gauge, using a flexible silicone rubber adhesive. Experience has shown that use of a more rigid adhesive means that the tag acts as a stress concentration and promotes premature failure in the specimen. Each gauge was connected to the signal processing equipment using a standard 3-wire lay-out. Use of this layout eliminates the effects of resistance changes in the lead wires. The gauges may have a reinforcing effect, producing a slightly stiffer specimen. The carrier for the gauge is an epoxy and thus it is felt that during the linear regime the reinforcing effects will be minimal. However, as the adhesive specimen yields the effect of the gauges will become more significant, leading to an overestimate of the stress calculated at a particular strain. This is consistent with the comparison between tensile and bending data (Fig. 4) which is discussed later.

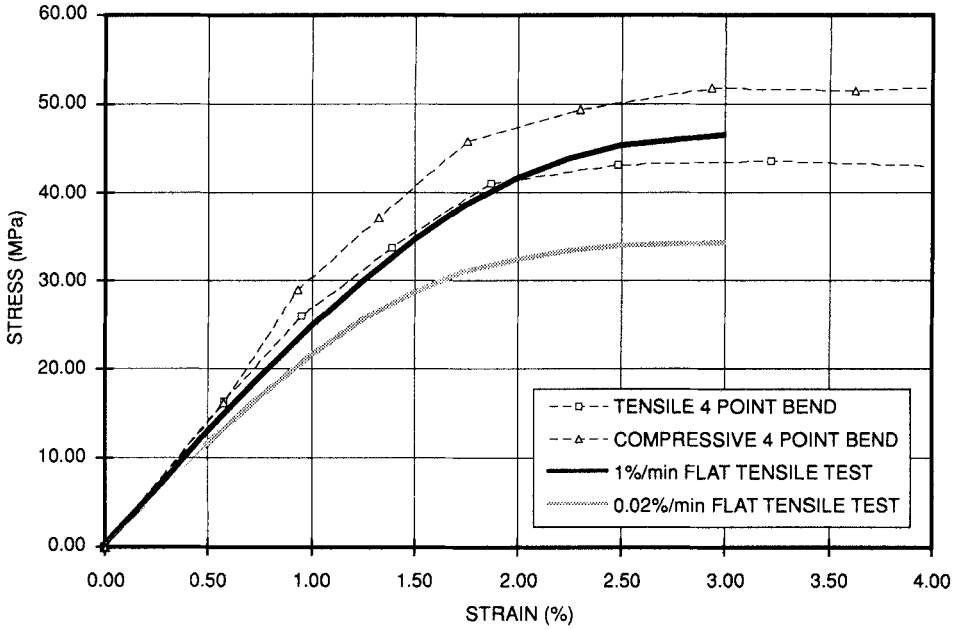

FIGURE 4 Adhesive tensile and compressive stress-strain curves.

PROCESSING OF RESULTS

The tests were carried out according to the procedure specified in the previous section and the load and surface strains were recorded. The way in which these data were processed is outlined below; in addition, results from one specific test are given in Table I to illustrate the procedure.

- The recorded force data (F) was converted into moment loading. At this stage, a correction was introduced that accounts for the reduction in the moment arm

TABLE I
Analysis of bend test data

M (Nmm/mm)	ϵ_t (%)	ϵ_c (%)	ω_t (mm)	ω_c (mm)	σ_t (MPa)	σ_c (MPa)	κ_t (%)	κ_c (%)	$S=\left\|\frac{\sigma_c}{\sigma_t}\right\|$	κ_t (MJ/m^3)	κ_c (MJ/m^3)	$S=\left\|\frac{\sigma_c}{\sigma_t}\right\|$
0.000	0.00	0.00	0.00	0.00	0.00	0.00	0.00	0.00	—	0.00	0.00	—
99.43	0.57	−0.58	3.02	3.03	16.3	−16.3	0.00	0.00	—	0.00	0.00	—
165.1	0.95	−0.93	1.21	1.14	26.0	−29.0	0.94	0.92	1.13	0.28	0.30	1.08
229.4	1.39	−1.32	0.97	0.88	33.8	−37.1	1.37	1.31	1.14	0.44	0.47	1.07
288.0	1.87	−1.76	0.81	0.73	41.0	−45.9	1.86	1.74	1.14	0.65	0.67	1.09
339.4	2.48	−2.30	0.77	0.68	43.2	−49.3	2.47	2.28	1.16	0.91	0.94	1.13
374.3	3.22	−2.93	0.72	0.62	43.6	−51.8	3.20	2.92	1.18	1.23	1.27	1.18
394.4	4.05	−3.63	0.65	0.55	42.9	−51.5	4.03	3.61	1.21	1.58	1.63	1.20
403.8	4.93	−4.34	0.58	0.47	41.0	−52.2	4.91	4.32	—	1.76	1.82	—

caused by the rotation of the specimen around the semi-circular anvils. To a first approximation, this can be expressed in terms of the crosshead displacement (Δ), the horizontal separation (D) of the two anvils, the radius (R) of the anvil and the specimen width and thickness (W and t, respectively) as

$$M = \frac{F}{2W}\left[\left(D - \frac{2R\Delta}{D}\right) - \frac{\Delta}{D}(t - \Delta)\right] \tag{18}$$

- The data points are then divided into groups and average moment and strain data are obtained for each group. This produces a smoothed set of data for use in reconstitution of the stress-strain curves. The data so obtained are shown in the first three columns of Table I. Only nine groups were used for brevity in this paper. It is necessary to have enough points to define clearly the shape of the final stress-strain curve. However, if the data are not averaged then the resulting curve oscillates about the curves obtained using averaged data. An optimum number of averaged groups has been found to be about 20. It is, however, necessary to have a sufficient number of data points in each group to enable averaging to be carried out effectively. In this work a total of about 1500 data points was recorded for each test.
- The widths of the regions that are subject to tensile and compressive stresses are then found using equations 11 and 12 and this is shown in columns 4 and 5 of Table I.
- Equations 9 and 10 are then used to find a solution for the first averaged data set. In this first increment all the values for the previous increment are taken as zero. This will produce an elastic solution (with different moduli in tension and compression if the surface strains are different). Solution of these equations gives the surface stresses corresponding to the measured surface strains. This is shown in the second row of columns 6 and 7 in Table I.
- Equations 9 and 10 are again solved this time for the next averaged data set. This is repeated until the final increment of loading is obtained and the data so obtained are shown in the remainder of columns 6 and 7 of Table I. In this manner a piecewise linear approximation to the tensile and compressive stress-strain curves can be found. These curves for the specimen used in the example above are shown in Figure 4. These can be compared with data obtained from standard tensile tests. The method of obtaining these data is discussed in the next section.
- Having evaluated the tensile and compressive stresses at each increment of loading it is then possible to use equations 13 and 15 to evaluate the corresponding hardening parameters. These are shown in Table I, columns 8 and 9 for strain hardening and columns 11 and 12 for work hardening. Linear interpolation can then be used to find the compressive and tensile stresses at the same hardening parameter and the ratio of these flow stresses (S) can be evaluated. This data reduction is shown in column 10 for strain hardening and column 13 for work hardening.

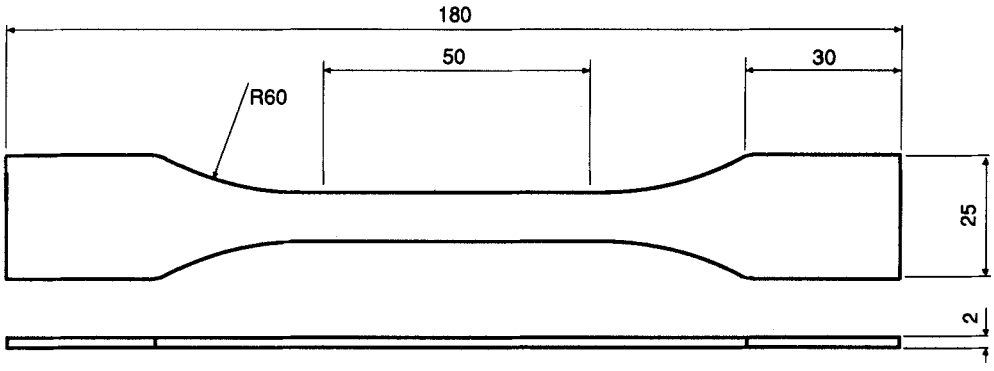

ALL DIMENSIONS IN MILLIMETRES

FIGURE 5 The bulk tensile test specimen.

STANDARD TENSILE TESTING

The tensile test specimen shown in Figure 5 is derived from BS2782, part 3. These are manufactured using a similar procedure to that employed when manufacturing the four-point bend specimens and have the same high quality surface finish. This is important, as a tensile test is much more prone to premature failure than the bend test. The specimens are placed in the wedge grips of the same Instron test machine and clip extensometers are attached to the gauge length, having earlier given the sections of the specimen that are directly under the extensometer knife edges a protective coating of varnish. The test machine is run in closed-loop mode, using the output from the extensometer to control the speed of the test machine such that the specimen experiences a constant strain rate.

In this way the stress-strain curve of the adhesive can be found as a function of strain rate. This testing forms part of a larger programme of testing which involves both creep and relaxation of the adhesive in question. The tests were carried out in a carefully controlled environment and, hence, excellent repeatibility was found for different specimens tested at the same strain rate. Due to the strain rate sensitivity of the adhesive, tests have been carried out at different rates and the two curves most relevant to this work have been plotted on Figure 4, along with the tensile and compressive curves from the four point bend specimen.

DISCUSSION

When comparing tensile curves from the four-point bend and flat tensile tests two points, concerning the rate of testing in the former, should be made. The surface strain rate is not constant and the strain rate varies through the thickness. The former effect is because the bend test has been carried out at a constant crosshead speed and the non-linearities in the system (which include rotation of the specimen on the anvils, local yielding and a gradual shifting of the neutral axis towards the compressive surface) mean that this does not result in a constant strain rate. It

should also be noted that the correction for rotation and friction of the specimens on the anvils will be quite complex and will tend to introduce tensile forces as well as affecting the applied moment. These effects are not fully accounted for in the analysis. However, Figure 4 shows that the tensile curve obtained from the bend specimen compares very favourably with data obtained from tensile tests at rates that straddle the surface strain rates actually obtained from the bend tests. It would be possible to control the Instron in a closed loop mode from the surface-mounted strain gauges to ensure a constant strain rate and this is likely to improve the accuracy still further. The stiffer response from the bending test could, in part, be attributable to the reinforcing effects of the strain gauge. This stiffening effect could be either eliminated (through the use of non-contacting extensometers), reduced (through the use of more compliant strain gauges) or accounted for in the analysis. This aspect is outside the scope of this current paper but can be addressed in future work, along with the effect of the strain rate.

Another important feature about the curves obtained from the bend tests is that they give data over a much larger range of strain than the tensile specimens. None of the bend specimens actually failed during the tests; the limitation reached was the setting on the strain gauge instrumentation which was set arbitrarily to 5% strain. By using high extension gauges it should be possible to obtain stress-strain data well in excess of this value. This is in contrast to the data from the tensile test, where the maximum measured strains for this adhesive were only of the order of 3.5–4%, even though considerable care was taken during specimen manufacture and testing.

Considering results displayed in Figure 4 further, it can be seen that the form of the tensile and compressive stress-strain curves have a similar shape, with the compressive curve showing a higher flow stress than the tensile curve. This is as expected, the hydrostatic compression suppressing yielding of the adhesive. As is typical with such polymers there is no clear point of yield but simply a gradual reduction in the slope of the curve. The ratio of compression to tension flow stresses can be seen to be fairly constant, Table I, settling to a value of 1.2. This is of the same order of magnitude as values obtained for other adhesives, specifically a value of 1.4[6] for a toughened adhesive and a more general value of 1.3.[1] The value that is obtained depends on which points on the tensile and compressive stress-strain curves are used to calculate the value of S. In this work, we consider the ratio to be evaluated at points of either equivalent strain hardening or equivalent work hardening. The value cited by Gali *et al.*[6] has been determined by assuming equal secant moduli for tension and compression. If equivalent strain or work hardening were used then a lower value would be obtained.

CONCLUSION

A well-established materials test technique, the four-point bend test, has been applied in a novel way to determine the tensile and compressive stress-strain curves and the compressive-to-tensile ratio of flow stresses for a specific adhesive. The technique works because, unlike metals, as yielding occurs the strains on the upper and lower surfaces of the strip become more and more disparate. This is because

yielding is suppressed on the compressive face. The test has been analysed and an incremental formula that can be used to reconstitute the two stress-strain curves from the moment-strain data has been presented. The actual test has been shown to offer a number of advantages over other tests. These include a much simpler specimen geometry, the replacement of two separate tests with a single test and an ability to generate tensile data over a much wider range than is currently possible with the existing tensile tests.

The results that were obtained from this new test procedure were compared with data from tensile tests and from other sources and a good match has been found, indicating that practically, as well as theoretically, this test is a worthy alternative to the existing tests. It has shown that the ratio that is required to implement a modified yield criterion for structural adhesives is essentially constant over the complete plastic range. This justifies the commonly-accepted procedure of using a constant value for this parameter in non-linear stress analyses.

Acknowledgements

The authors would like to thank Alcan International, Permabond Ltd and the SERC for the support they have given during the period this work was carried out.

Appendix

This section indicates how incremental equations 9 and 10 are derived. Consider a section through the centre part of the four-point bend specimen at loading increment i. The stress and strain distributions across this section are shown in Figure 6. The

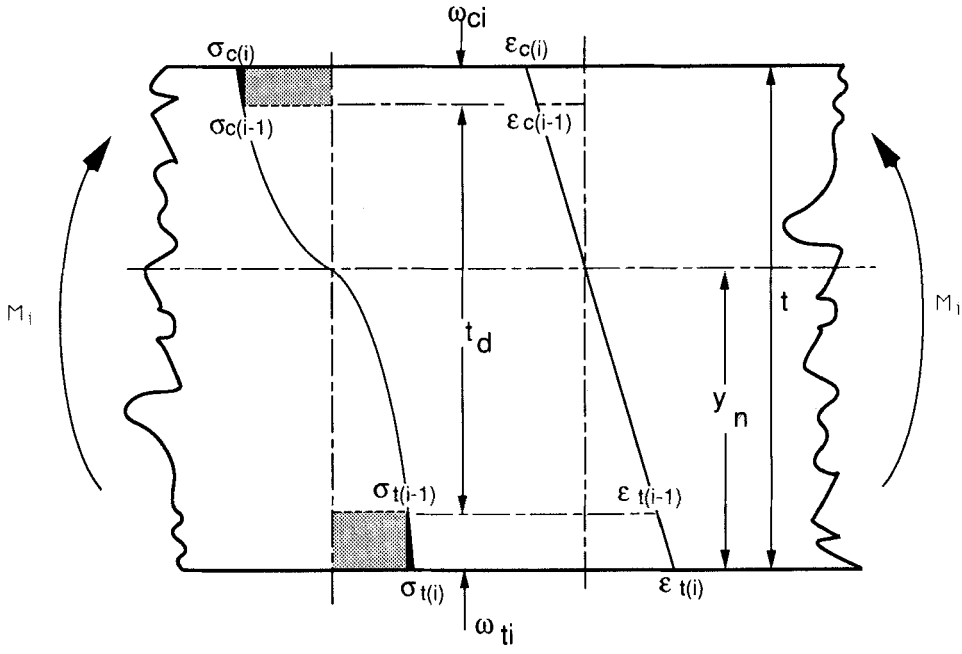

FIGURE 6 Stress and strain distributions through the thickness of the bend specimen.

section can be divided into two parts; an inner part of depth, t_d which ends where the tensile and compressive strains equal the surface strains recorded in the previous loading increment (*i.e.* region of defined material behaviour) and an outer part which constitutes the remainder of the section. The depth of this outer part is ω_{ti} and ω_{ci} on the tensile and compressive sides, respectively. These depths can be found by assuming a linear distribution of strains across the section and appropriate expressions are given in equations 11 and 12.

Now, the total moment, M_i, is the sum of the moment carried by the inner and outer parts. It can be shown that if the uniaxial stress is a function of strain only, the moment carried by a strip with fixed surface strains is simply proportional to the square of the thickness of the strip. Thus, the moment carried by the inner section can be expressed in terms of the total moment at the last increment (M_{i-1}) and the moment carried by the outer sections of undefined material behaviour (M_u) can be written as

$$M_u = M_i - M_{i-1}\left[\frac{t_d}{t}\right]^2 \tag{A1}$$

Similarly, the tension carried by the region of undefined material behaviour (T_u) can be shown to be

$$T_u = T_i - T_{i-1}\left[\frac{t_d}{t}\right] \tag{A2}$$

The moments and tension carried by the regions of undefined material behavior can also be expressed in terms of the stress integrals similar to equations 6 and 7 but integrated only across the region of interest. If, as a first approximation, the undefined stress-strain behaviour is assumed to be linear, these equations can be integrated over the outer part of the section, *i.e.* across ω_{ti} and ω_{ci} giving the equation below (refer to Figure 6 for clarification).

$$\begin{aligned} M_u = {} & \sigma_{ti-1}\omega_{ti}\cdot\left[y_n - \frac{\omega_{ti}}{2}\right] + (\sigma_{ti} - \sigma_{ti-1})\frac{\omega_{ti}}{2}\cdot\left[y_n - \frac{\omega_{ti}}{3}\right] \\ & - \sigma_{ci-1}\omega_{ci}\cdot\left[t - y_n - \frac{\omega_{ci}}{2}\right] - (\sigma_{ci} - \sigma_{ci-1})\frac{\omega_{ci}}{2}\cdot\left[t - y_n - \frac{\omega_{ci}}{3}\right] \end{aligned} \tag{A3}$$

$$T_u = \frac{(\sigma_{ti} + \sigma_{ti-1})}{2}\omega_{ti} + \frac{(\sigma_{ci} + \sigma_{ci-1})}{2}\omega_{ci} \tag{A4}$$

Combining and rearranging equations A1–A4 yields the following two equations expressing the moment and tensile force carried by the specimen in increment i.

$$\begin{aligned} M_i = {} & M_{i-1}\left[1 - \frac{\omega_{ti} + \omega_{ci}}{t}\right]^2 + \sigma_{t(i-1)}\omega_{ti}\left[\frac{y_n}{2} - \frac{\omega_{ti}}{3}\right] - \sigma_{c(i-1)}\omega_{ci}\left[\frac{t - y_n}{2} - \frac{\omega_{ci}}{3}\right] \\ & + \sigma_{ti}\frac{\omega_{ti}}{2}\left[y_n - \frac{\omega_{ti}}{3}\right] - \sigma_{ci}\frac{\omega_{ci}}{2}\left[t - y_n - \frac{\omega_{ci}}{3}\right] \end{aligned} \tag{A5}$$

$$T_i = T_{i-1}\left[1 - \frac{\omega_{ti} + \omega_{ci}}{t}\right] + \sigma_{t(i-1)}\frac{\omega_{ti}}{2} + \sigma_{c(i-1)}\frac{\omega_{ci}}{2} + \sigma_{ti}\frac{\omega_{ti}}{2} + \sigma_{ci}\frac{\omega_{ci}}{2} \tag{A6}$$

Noting that the tensile force carried by the specimen is zero, the above equations can be solved for σ_{ti} and σ_{ci} to provide the pair of equations 9 and 10 in the main text.

References

1. J. A. Harris and R. D. Adams, *Int. J. Adhesion and Adhesives* **4,** 65 (1984).
2. D. A. Bigwood, A. D. Crocombe, *Int. J. Adhesion and Adhesives* **10,** 31 (1990).
3. R. B. Kreiger, "Stiffness characteristics of structural adhesives for stress analysis in a hostile environment," American Cyanamid Company, Havre de Grace, MD, USA, 1975.
4. R. S. Raghava and R. M. Cadell, *J. Mat. Sci.* **8,** 225 (1973).
5. N. A. Peppiat, "Some aspects of the paraboloidal yield surface," University of Bristol Internal Report, 1976.
6. S. Gali, G. Dolev and O. Ishai, *Int. J. Adhesion and Adhesives* **1,** 135 (1981).
7. C. W. Richards, *Engineering Materials Science* (Chapman and Hall, New York and London, 1961), pp. 167–184.